SCIENCE CHINA
Earth Sciences

•ARTICLE•

July 2023 Vol.66 No.7: 1468–1477
https://doi.org/10.1007/s11430-022-1079-5

Temperature variations along the Silk Road over the past 2000 years: Integration and perspectives

Jianhui CHEN[1*], Haipeng WANG[2], Yan LIU[1], Shuai MA[1] & Wei HUANG[1]

[1] *MOE Key Laboratory of Western China's Environmental Systems, Lanzhou University, Lanzhou 730000, China;*
[2] *State Key Laboratory of Cryospheric Science, Northwest Institute of Eco-Environment and Resources, Chinese Academy of Sciences, Lanzhou 730000, China*

Received September 22, 2022; revised February 2, 2023; accepted February 21, 2023; published online June 14, 2023

Abstract Reconstructing temperature changes along the Silk Road (SR) over the last two millennia can provide insights into past global changes and their impact on the rise and fall of ancient civilizations in this region. Numerous high-quality single-site paleotemperature records have been produced for the eastern part of the SR (mainly for the Xinjiang region and its surrounding areas), which provide the data basis for a comprehensive synthesis. In this study, we used objective criteria to select 10 high-quality ones from 30 temperature reconstructions derived from various geological archives including lacustrine sediments, ice cores, and tree rings in this region. Our aims are to summarize the pattern of temperature change over the past 2000 years, to provide a long-term viewpoint on the present warming, and to evaluate the impact of climate change on civilizations along the SR. The principal results are as follows: (1) The temperature variations over the last millennium are mutually consistent within these records. The study area experienced typical climate anomalies during the Medieval Warm Period (MWP, AD 1000–1250), the Little Ice Age (LIA, AD 1450–1850), and the Current Warm Period (CWP, AD 1850 to present); however, contrary to previous knowledge, the amplitude of climatic warming during the CWP did not exceed that during the MWP. (2) Fewer temperature records were available for the interval AD 1–1000, and there were large differences between them. For example, the reconstructed climate during both the Han Dynasty and the Sui-Tang Dynasties was either warm or cold, without prevailing consensus. (3) The warming during the MWP favored the rapid development of the SR route along the northern slopes of the Tianshan Mountains, and the cooling during the LIA contributed to the decline of the SR marked by the closure of the Jiayuguan Pass. Notably, the scarcity of temperature records and the discrepancies between them during AD 1–1000 in the eastern part of the SR have hindered our understanding of the hydroclimatic changes and their influence on the development of civilizations along the SR. Thus, it is important to obtain an increased number of high-quality reliable records spanning the past 2000 year, and to examine the occurrence of local signals of temperature changes during the period of AD 1–1000. On the other hand, the paleotemperature investigation on the western part of the SR over the last two millennia is wholly insufficient, and thus more high-quality single-site and integrated studies are needed, to facilitate more comprehensive insights into the coupled relationship between climate change and the rise and fall of civilizations along the entire length of the Silk Road.

Keywords Silk Road, Medieval Warm Period, Little Ice Age, Current Warm Period, Rise and fall of civilizations

Citation: Chen J, Wang H, Liu Y, Ma S, Huang W. 2023. Temperature variations along the Silk Road over the past 2000 years: Integration and perspectives. Science China Earth Sciences, 66(7): 1468–1477, https://doi.org/10.1007/s11430-022-1079-5

1. Introduction

The ancient Silk Road (SR), which was initiated during the Western Han Dynasty (202 BC–AD 8), opened a channel for commercial trade and technological communication between East and West, and it also facilitated trans-continental cultural exchanges. Knowledge of the temperature changes over

* Corresponding author (email: jhchen@lzu.edu.cn)

the past 2000 years is crucial for understanding the coupled relationship between climate change and the rise and fall of ancient civilizations along the Silk Road. Moreover, the region within which the SR lies is a constituent part of arid central Asia, featuring a high sensitivity to global climate changes. It is suggested that the temperature increases in this arid region over the past century were significantly higher than the global average (Huang et al., 2017). However, it remains unclear whether this remarkable anthropogenic warming has exceeded the natural climatic variability, and a comprehensive integration based on high-quality single-site paleotemperature records is an effective means of addressing this question.

Over the past 10 years or so, an increased number of high-quality single-site paleotemperature records from along the SR have been produced (e.g., Liu et al., 2014; Zhang et al., 2014; Büntgen et al., 2016), providing the basis for a comprehensive synthesis. Most of these records are from the Xinjiang region (NW China) and surroundings, which hosts the main part of the eastern SR (Figure 1a, 1b), and thus it falls within the spatial scope of this study. Notably, several large-scale researches of temperature evolution during the past millennium, mainly using tree rings, have been produced for this region (Figure 1b). For example, the temperature reconstruction for 'Northwest China' during AD 850–2000 by Ge et al. (2013) was based on two tree-ring chronologies from the central Qilian Mountains. As another example, Zhang H et al. (2018) and Liu et al. (2021) reconstructed the temperature changes in 'Northwest China-western Mongolia' and 'Northwest part of East Asia' over the past 1200 years, respectively, using a same set of proxy records. As far as records with a length of or more than 1000 years in our study area are concerned, Zhang H et al. (2018) used an ice-core oxygen isotope profile from the Qilian Mountains and a tree-ring record from western Mongolia, while Liu et al. (2021) only used the latter. Although the eastern part of the SR was not the primary focus of this research, the results show that our study area did not experience significant climatic anomalies during the Medieval Warm Period (MWP, AD 1000–1250) and the Little Ice Age (LIA, AD 1450–1850), but that remarkable warming occurred during the Current Warm Period (CWP, AD 1850 to present) which exceeded that of the MWP. These investigations make an important contribution to a deeper understanding of temperature changes in the study area over the last millennium. However, considering the amount of available material at that time and the characteristics of the prevailing tree-ring proxy itself, these earlier studies—in terms of their relevance to the area of interest in the present study—were limited in spatial coverage and temporal duration, in intercomparison and integration of multiple indicators, and in the extraction of low-frequency signals.

In this study, we first compiled an up-to-date set of temperature records obtained from different geological archives in Xinjiang and its surroundings (more than three-quarters of which were published in the last 10 years). Then, based on effective quality control, we conducted a systematic comparison and integration of these records. After that, we summarized the general characteristics of temperature change in the eastern part of the SR over the last two millennia, provided a long-term perspective on the current warming of this region, and evaluated the possible influence of climate change on human activities in two iconic historical events. Finally, we reviewed the prospects for future research on temperature changes along the Silk Road during the past 2000 years.

2. Materials and methods

We collected an initial total of 30 paleotemperature records spanning at least the past 1000 years from 19 sites (Figure 1b) in the study area (see Table 1 for detailed information). Two screening criteria were then applied to these sites: (1) there was at least one age control point every 500 years, on average (including records based on annual laminae, of course); and (2) the resolution was better than 30 years. When multiple temperature records were available for the same site, the most recently published record was selected. A total of 10 paleo-temperature records (Figure 2a–2j) meeting these criteria were then subjected to a comprehensive analysis. These records are based on different proxies from various geological archives. They include four tree-ring width chronologies (Esper et al., 2002, 2003; Zhang et al., 2014; Büntgen et al., 2016), two ice-core oxygen isotope records (Yao et al., 1996; Thompson et al., 2006), and four physicochemical records from lake sediments (He et al., 2013; Liu et al., 2014; Lan et al., 2018). Among these ten records, five records reflected summer temperature changes (T2, T9, T11, T12, T17), one record reflected temperature variations from January to August (T13), one record revealed mean annual temperature fluctuations (T18), and the other three records lacked a clear temperature seasonality signal (T14, T15, T19). Based on CRU TS v4.05 (Harris et al., 2020), the summer temperature variations during the observation period in the study area are significantly correlated with changes in mean annual temperature (R=0.75, p<0.01, figure omitted). The physicochemical proxies from lake sediments (T14) and the ice-core oxygen isotope records (T15, T19) typically contain an annual temperature signal. Thus, the integrated temperature record in this study can be used to indicate changes in annual mean temperature change.

Firstly, all the records were normalized to the 0–1 range. To facilitate comparative analysis and to identify any similarities among the proxy records on the multi-centennial scale, the normalized data were processed with a 200-year

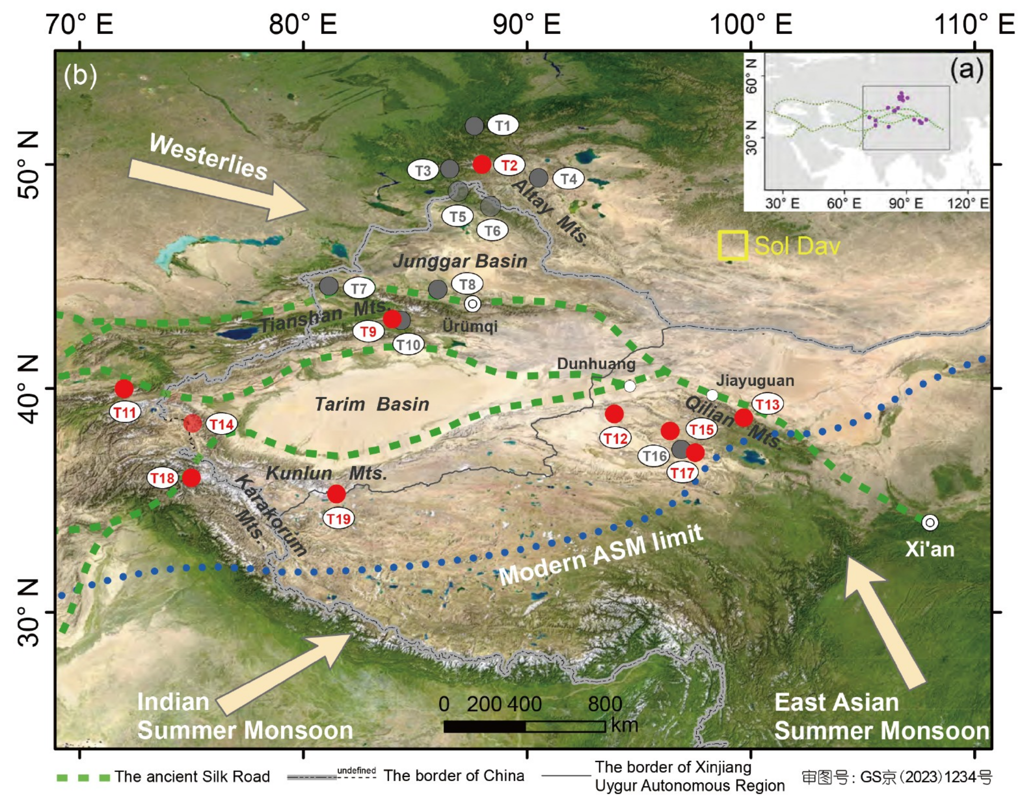

Figure 1 Distribution of the temperature records spanning at least the past 1000 years along the Silk Road and surroundings. (a) Study area in the Eurasian Continent. The rectangle indicates the eastern part of the SR. (b) Location of paleotemperature records collected in this study (T1–T19, see Table 1 for detailed information). The red dots represent the sites of the 10 high-quality records. The records used by Ge et al. (2013), Zhang H et al. (2018), and Liu et al. (2021) are from T13, T15 & Sol Dav, and Sol Dav, respectively. The modern Asian summer monsoon (ASM) limit was modified from Chen et al. (2010).

low-pass forward-backward filter. Then, the normalized data, for the period of good coherence, were averaged using an arithmetical mean to achieve integration. Finally, this integrated record was compared with instrumental data over the past century in the study area (CRU TS v4.05, Harris et al., 2020) to evaluate its reliability. The integrated record, as the essential data, will be used to analyze the general characteristics of temperature change, to identify the position of the CWP in the context of long-term temperature fluctuation, and to evaluate the impacts of climate change on the civilizations along the SR.

3. Results and discussion

(1) Due to the limitations of its age control and resolution, our integrated record cannot be calibrated year-by-year using observational data. However, this record is in good agreement with the observed mean annual temperature over the past 100 years in the study area (Figure 3a), supporting its overall reliability. During the last millennium, most of the research sites in the eastern part of the SR experienced significant temperature anomalies during the MWP (AD 1000–1250), the LIA (AD 1450–1850), and the CWP (AD 1850 to present), indicating that the temperature variations within the study area were consistent (Figure 2k). Moreover, the integrated record is coherent with the temperature reconstruction for East China based on documentary evidence (Figure 2l, Ge et al., 2003), and with multi-proxy-based temperature reconstructions for China (Figure 2m, Yang et al., 2002) and the Northern Hemisphere (Figure 2n, Moberg et al., 2005), on the centennial scale. It is worth noting that our result is different from the existing temperature integrations for this region (Figure 3). Multiple studies based mainly on limited tree rings show no clear temperature trend during AD 1000–1850, and there were no significant temperature anomalies during the MWP and the LIA (Ge et al., 2013, Figure 3b; Zhang H et al., 2018, Figure 3c; Liu et al., 2021, Figure 3d). Our findings suggest that the particularity of the temperature history of this arid region over the past millennium, indicated by the previous studies, needs to be reexamined. Interestingly, all these records show synchronous changes on interdecadal time scales, such as the warm-to-cold phase transition in the late 13th century, and the cold-to-warm phase transition in the mid-19th century (Figure 3). This emphasizes the accuracy of tree ring records for reflecting high-frequency signals of climate change.

Although there is a recent large warming trend in the study

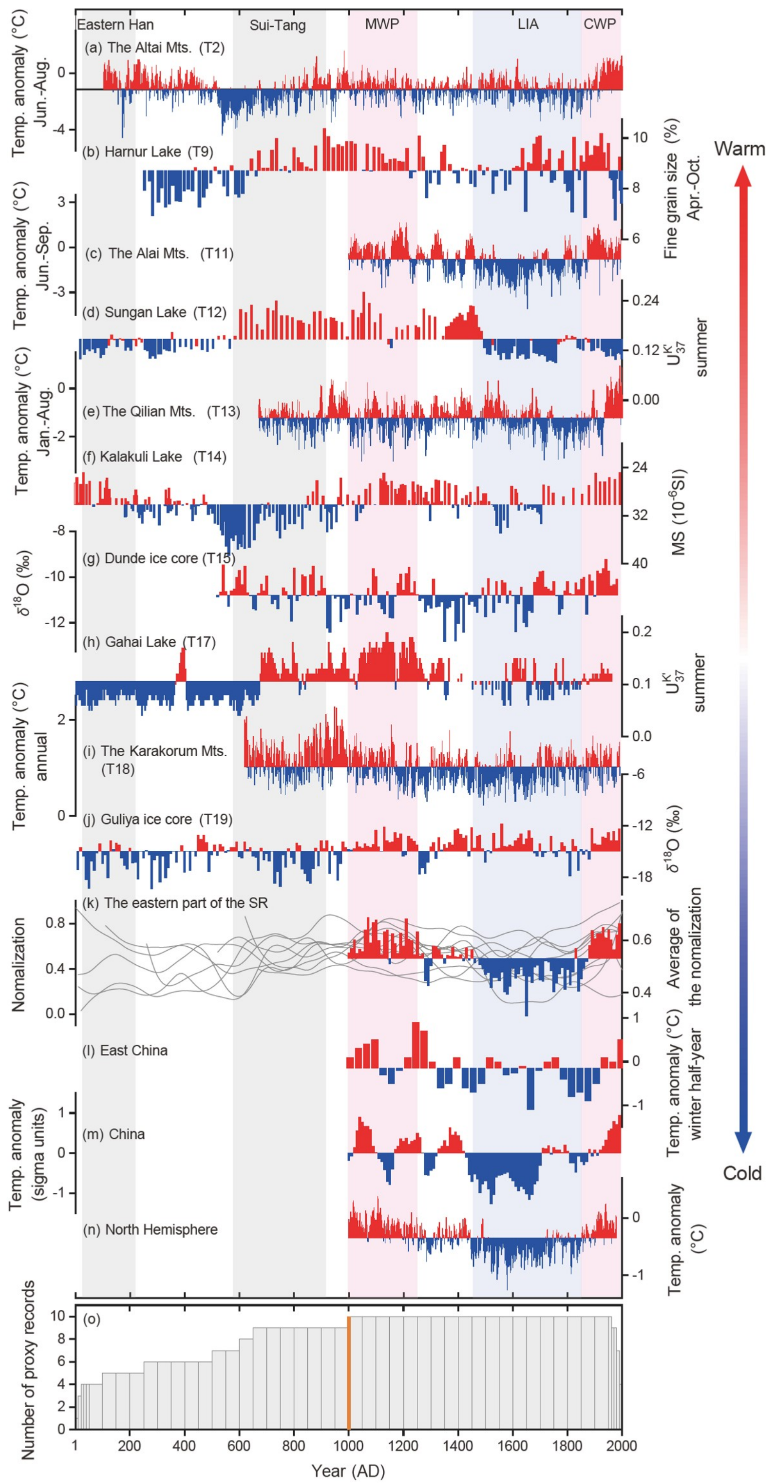

Figure 2 High-quality temperature records from the eastern part of the SR and their integration over the past millennium, and their comparison with temperature reconstructions from other regions. (a) Tree-ring width from the Altai Mountains (T2, Büntgen et al., 2016); (b) Grain-size record from Harnur Lake (T9, Lan et al., 2018); (c) Tree-ring widths from the Alai Mountains (T11, Esper et al., 2003); (d) Alkenone indices from Sugan Lake (T12, He et al., 2013); (e) Tree-ring widths from the central Qilian Mountains (T13, Zhang et al., 2014); (f) Magnetic susceptibility record from Kalakuli Lake (T14, Liu et al., 2014); (g) δ^{18}O from the Dunde ice core (T15, Thompson et al., 2006); (h) Alkenone indices from Gahai Lake (T17, He et al., 2013); (i) Tree-ring widths from the northwestern Karakorum Mountains (T18, Esper et al., 2002); (j) δ^{18}O record from Guliya ice core (T19, Yao et al., 1996; Thompson et al., 1997); (k) 200-year low-pass filter results of the 10 normalized records (gray lines) and the average of the 10 normalized records over the past 1000 years (bars); Temperature reconstructions for East China based on historical documents (l) (Ge et al., 2003), for China based on multiple proxies (m) (Yang et al., 2002), and for the Northern Hemisphere based on multiple proxies (n) (Moberg et al., 2005). Each of the above records is compared to their average for the period they cover, with values higher than the average shown as red bars, and values lower than the average shown as blue bars. The bar chart at the bottom (o) shows the number of proxy records used in this study for different periods. Note the significant decreasing trend from AD 1000 backwards.

Table 1 Paleotemperature proxy records spanning at least the last 1000 years in the eastern part of the SR

Site no.[a)]	Site name	Latitude	Longitude	Altitude (m asl)	Time period	Dating material	Dating method	No. of dates[b)]	Sample resolution (yr)[c)]	Proxies	Seasonality[d)]	Reference
T1	Lake Teletskoye	51.72°N	87.65°E	1900	1000 BC–AD 2006	Wood fragment and remains of moss	^{210}Pb/^{137}Cs, ^{14}C	3/3	~5	Br, Ti, XRD, Sr/Rb	Annual	Kalugin et al., 2009
					2150 BC–AD 2006				~5–25	Geochemical features and pollen records	NA	Babich et al., 2015
					2150 BC–AD 2006				~25–40	Pollen	The warmest month	Rudaya et al., 2016
T2	**Russian Altai-Sayan Mountains**	**45°–50°N**	**85°–90°E**	**2100–2500**	**AD104–2011**	–	**Tree-ring counting**	–	**1**	**Tree-ring width**	**Jun.–Aug.**	Büntgen et al., 2016
					359 BC–AD 2007					Tree-ring width	Jun.–Jul.	Myglan et al., 2012a
					AD 536–2006					Tree-ring width	Jun.–Jul.	Myglan et al., 2012b
T3	Belukha ice core	49.8°N	86.55°E	4115	11,170 BC– AD 2003	Particulate organic carbon	Steady-state glacier flow model and ^{14}C radiocarbon	1/4	~7	δ^{18}O	Annual	Aizen et al., 2016
T4	Achit Nuur	49.42°N	90.52°E	1444	~22,600–0 cal BP	Bulk sediment	^{14}C	3/10	~250	Pollen	Annual	Sun et al., 2013
T5	Tielishahan peat bog	48.81°N	86.92°E	1770	~9.7–0 cal kyr BP	Plant macrofossils, bulk peat and wood residues	^{14}C	1/5	~120	Pollen	NA	Zhang Y et al., 2018
	Narenxia peatland	48.8°N	86.9°E	1760	~11,500–0 cal yr BP	Peat and lake mud	^{14}C	2/11	~60–70	Pollen	Annual, warm and cold season	Feng et al., 2017
	Narenxia peatland	48.8°N	86.92°E	1763	~7.7–0 kyr BP	Plant residue and woody remains	^{14}C	4/13	~60–70	brGDGTs	NA	Rao et al., 2020a
T6	Kelashazi Peat	48.12°N	88.37°E	2422	~4100–0 cal yr BP	Plant residuals	^{14}C	2/4	~80	Pollen	NA	Zhang et al., 2020
	Sahara sand wetland	48.12°N	88.36°E	2450	~11–0 kyr BP	Peat α-cellulose samples	^{14}C	3/22	~45	α-cellulose δ^{13}C	Summer	Rao et al., 2019
										α-cellulose δ^{18}O	Winter	Rao et al., 2020b
	Sahara sand wetland	48.11°N	88.36°E	2446	~11–0 kyr BP	Bulk peat samples	^{14}C	1/11	~100	brGDGTs	Annual	Wu et al., 2020
T7	Sayram Lak	44.58°N	81.15°E	2071.9	~9.6–0 cal ka BP	Bulk organic matter	^{14}C	1/12	~50	Pollen	NA	Jiang et al., 2013
T8	Caotanhu wetland	44.42°N	86.02°E	380	~4000–0 cal a BP	Bulk sediments	^{14}C	2/5	~30	Pollen	Annual	Zhang et al., 2015
T9	**Harnur Lake**	**43.11°N**	**83.97°E**	**2941**	**AD~300–2000**	**Bulk organic matter**	**^{210}Pb/^{137}Cs,^{14}C**	**4/4**	**~12**	**Fine grain-size fraction**	**Ice-free seasons (Apr. to Oct.)**	Lan et al., 2018
T10	Swan Lake	43.05°N	84.38°E	2541	~8.5–0 ka BP	Organic matter	^{14}C	3/8	~170	Pollen	NA	Huang et al., 2015
T11	**Alai Range of the western Tien Shan**	**39.83° –40.2°N**	**71.5°–72.62°E**	**2800–3400**	**AD1000–1995**	–	**Tree-ring counting**	–	**1**	**Tree-ring width**	**Jun.–Sept.**	Esper et al., 2003
T12	**Sugan Lake**	**38.87°N**	**93.9°E**	**2793**	**188 BC–AD 2006**	**Bulk organic matter**	**^{210}Pb/^{137}Cs,^{14}C**	**5/5**	**~11–33**	$U^{K'}_{37}$	**Summer**	He et al., 2013
					0–AD 1950	Seed and plant remain	^{210}Pb/^{137}Cs, ^{14}C	4/6	~30–40	δ^{13}C	Winter half year	Qiang et al., 2005
T13	**Northern slope of the central Qilian Mountains**	**38.69°–38.72°N**	**99.67°–99.7°E**	**3300–3578**	**AD670–2012**	–	**Tree-ring counting**	–	**1**	**Tree-ring width**	**Minimum temperature from Jan. to Aug.**	Zhang et al., 2014
	Central Qilian Mountains-Sidalong	38.4°N	99.9°E	3400–3550	AD 1000–2000	–	**Tree-ring counting**	–	1	Tree-ring width	Dec.–Apr.	Liu et al., 2005
T14	**Kalakuli Lake**	**38.44°N**	**75.06°E**	**3645**	**2223 BC–AD 1992**	**Organic matter**	**^{14}C**	**11/17**	**~5**	**Magnetic susceptibility, grain size, elements**	**NA**	Liu et al., 2014
T15	**Dunde ice core**	**38.1°N**	**96.4°E**	**5325**	**520–1987AD**	–	**Annual layer counting & ice flow model**	–	**10**	**δ^{18}O**	**NA**	Thompson et al., 2006
T16	Hurleg Lake	37.28°N	96.9°E	2817	~9000–0 cal yr BP	Aquatic plant leaves	^{14}C	5/11	~45	$U^{K'}_{37}$	Summer	Zhao et al., 2013
T17	**Gahai Lake**	**37.13°N**	**97.52°E**	**2848**	**624 BC–AD 1962**	**Bulk organic matter**	**^{210}Pb/^{137}Cs,^{14}C**	**4/4**	**~5**	$U^{K'}_{37}$	**Summer**	He et al., 2013
T18	**NW Karakorum**	**35°–37°N**	**74°–76°E**	**2700–3900**	**AD618–1993**	–	**Tree-ring counting**	–	**1**	**Tree-ring width**	**Annual**	Esper et al., 2002
T19	**Guliya ice core**	**35.28°N**	**81.48°E**	**6200**	**0–AD 1989**	–	**Annual layer counting & ice flow model**	–	**10**	**δ^{18}O**	**NA**	Yao et al., 1996; Thompson et al., 1997

a) Study sites are numbered in latitudinal order, from highest to lowest. b) Number of dates within the last two millennia/total dates in the sequence. ^{210}Pb/^{137}Cs dates are counted as one. c) Average temporal resolution over the last two millennia. If multiple proxies were available for the same site, the record with the highest resolution was selected. d) 'NA' indicates that the seasonality of the proxies was not specified in the original study. The 10 records selected for integration are shown in bold.

area, it cannot be concluded that its amplitude exceeds that of the earlier natural warm periods. Our integrated record demonstrates the occurrence of warmer-than-today periods within the MWP on the decadal timescale (Figure 2k), and that the average temperature on the centennial scale is at least comparable to that of the CWP (Figure 3a). This is clearly different from previous temperature integrations, which show that the amplitude of the current warming significantly exceeds that of the MWP (Figure 3b–3d). A modern climatological study indicates that the warming trend during 1920–2015 (1.94°C/96 yr) for the study area is 50% higher than the global average (1.23°C/96 yr), and that the mean warming may reach 3.2–4.0°C under the 2°C global warming scenario (Huang et al., 2017). This phenomenon is mainly attributed to the energy balance model of land-air interaction in arid and semi-arid regions (Huang et al., 2017). Our results imply that there may be a similar intensification of warming driven by natural factors in this region, and determining the mechanism responsible clearly requires further study.

(2) Compared with the past 1000 years, there are only four high-quality temperature records spanning the whole period of AD 1–1000 (Figure 2o). Furthermore, large discrepancies exist between them (Figure 2k). For example, the tree-ring record from the Altai Mountains indicates a warm climate during the Eastern Han Dynasty (AD 25–220) (Figure 2a), while the oxygen isotope record from the Guliya ice core indicates a cold climate for the same interval (Figure 2j). As another example, the sedimentary record from Sugan Lake in the western Qaidam Basin indicates a warm climate during the Sui-Tang Dynasties (AD581–907) (Figure 2d), while the record from Kalakuri Lake on the Pamir Plateau indicates a cold climate during this period (Figure 2f). More high-quality paleotemperature records are urgently needed to determine whether these discrepancies are the result of the local expression of temperature changes (i.e., the external forcings of the climate system were insufficient to drive synchronous change in temperature at these sites on the centennial scale), or they are the result of uncertainties in individual records themselves, such as the differences in seasonality and proxy sensitivity. Therefore, we did not carry out an integration for this period.

(3) The temperature fluctuations over the past 1000 years may have had important impacts on the rise and fall of civilizations in the eastern part of the SR. Here, we give two examples. First, the SR route along the northern slopes of the Tianshan Mountains (i.e., the new northern route of the SR) developed rapidly during the MWP under the control and operation of the 'Xizhou Uighurs' (Fu, 2019). Although many studies have indicated generally low precipitation/humidity during this period (e.g., Chen et al., 2010 and re-

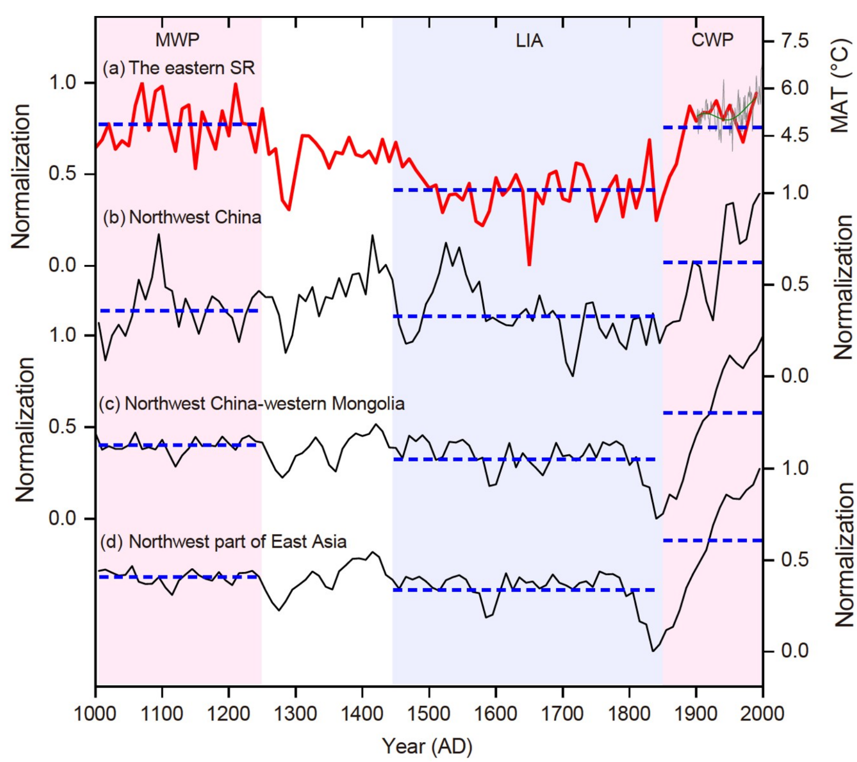

Figure 3 Comparison of the integrated temperature record for the eastern part of the SR over the past 1000 years with previous integrated records. (a) Integrated high-quality temperature record for the eastern SR (this study, red line) and observations of mean annual temperature in the study area since 1901 (CRU TS v4.05, Harris et al., 2020; the gray line indicates year-by-year temperature variations, and the green line is the result of 15-point FFT smoothing); (b) temperature record for 'Northwest China' (Ge et al., 2013); (c) temperature record for 'Northwest China-western Mongolia' (Zhang H et al., 2018); (d) temperature record for 'Northwest part of East Asia' (Liu et al., 2021). For comparison, all records are normalized, and their average values during the MWP, the LIA, and the CWP are plotted as blue dashed lines.

ferences therein), the increase in the snow- and ice-derived meltwater under high air temperatures (Figure 4a) may have provided a favorable environment for the rise of the 'Xizhou Uighurs', given that meltwater contributed more than precipitation to runoff in most of the catchments in the central Tianshan Mountains (Zhang et al., 2016; Yao et al., 2022). The increase in meltwater on the northern slopes of the Tianshan Mountains during the MWP has been verified by a runoff reconstruction from the Daxigou profile in this region (Figure 4b, Zhang et al., 2009). Second, the closure of the Jiayuguan Pass in AD 1539 is regarded as an iconic event of the decline of the SR (Zhou and Ding, 2006; Yong, 2015). The significant role of social and geopolitical factors, such as wars, frontier defense policy, and the evolution of regional strategic position in this event have been intensively discussed in previous studies (e.g., Chen, 2011; Ma, 2019). However, from a natural environmental point of view, the LIA cooling in the study area (Figure 4a) contributed to the formation of a strong wind field (Chen et al., 2013) and the intensification of aeolian activity (Huang et al., 2011; He et al., 2015; Zhou et al., 2019) (Figure 4c), and thus increased the difficulty in travel along the SR. Moreover, the lower temperatures would have decreased the meltwater supply and further accelerated the process of desertification and abandonment of Dunhuang, located in the throat place of the SR (Dong et al., 2021) (Figure 4d). All these factors may have caused the central government of the Ming Dynasty (AD 1368–1644) to cease the management and operation outside of the Jiayuguan Pass.

It is noteworthy that the significant discrepancies among the different temperature records during the period AD 1–1000 hamper our ability to explore the relationship between climate change and the vicissitudes of civilizations along the SR. The indiscriminate use of paleotemperature records may result in contradictory conclusions between different works. For example, a recent study based on cladocerans and historical documents showed a rapid decline in the water level of Boston Lake and the abandonment of ancient cities in the Tarim Basin during AD 280–450, which was dominantly attributed to decreased meltwater inputs caused by low temperature (Li et al., 2021). Similarly, another study based on remote-sensing image interpretation and stratigraphic dating also found a persistent decrease in the water level of Lop Nur, located in the lower reaches of Bosten Lake, during AD 360–470, and its disappearance at ~AD 500. However, contrary to the former study, the decline in the lake level of Lop Nur and the temporary demise of the Loulan Kingdom were attributed to increased evaporation resulting from high temperatures and a dry climate (Shao et al., 2022). Evidently, as an important aspect of hydroclimatic changes in the Tarim Basin, the water level fluctuations of Bosten Lake and its downstream Lop Nor showed similar patterns of decline during the 3rd–5th centuries AD, but which were ascribed to opposing temperature trends. This apparent contradiction

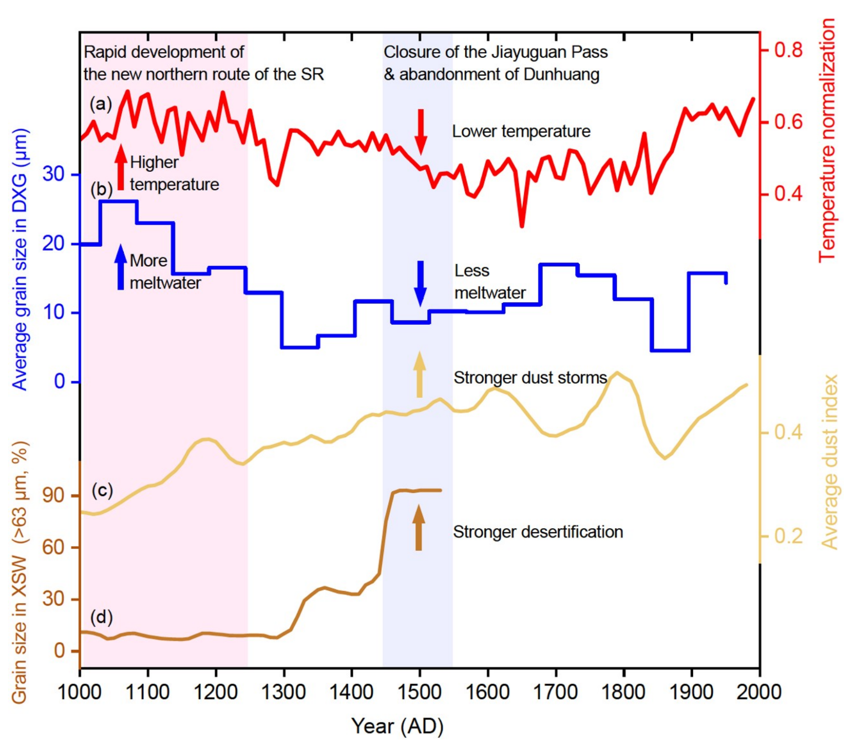

Figure 4 Impacts of temperature and the associated environmental factors on the rise and fall of the eastern SR civilization. (a) Integration of temperature records from the eastern part of the SR (this study); (b) Average grain size of Daxigou (DXG) profile on the northern slopes of the Tianshan Mountains (Zhang et al., 2009); (c) 50-year averaged synthesis of dust storms across mid-latitude Asia (He et al., 2015); (d) Sand fraction (>63 μm) record of the Xishawo (XSW) profile in Dunhuang (Dong et al., 2021). The pink and light blue shading indicates the MWP and the beginning of the LIA, respectively.

emphasizes that the lack of high-quality temperature records has already hindered the exploration of human-environment relationships during the historical period in the study area.

4. Conclusion and perspectives

We compiled 30 paleotemperature records spanning at least the past 1000 years in the eastern part of the SR, from which 10 high-quality records with a high temporal resolution and good age control were selected for integration and analysis. Our principal conclusions are as follows.

(1) The paleotemperature records over the past 1000 years are in good agreement with each other. The study area experienced typical climate anomalies during the MWP, the LIA, and the CWP. Notably, the amplitude of the warming during the CWP did not exceed that during the MWP. These characteristics differ substantially from the previous knowledge obtained mainly through limited tree-ring records, which suggested low-amplitude temperature fluctuations during the MWP and the LIA and significant warming during the CWP.

(2) There are few records available for the study area that span the period of AD 1–1000, and there are large discrepancies between them, which impedes further exploration of hydroclimatic changes in the eastern part of the SR and their influence on the rise and fall of human civilizations in this region.

(3) Increased water supply from melting snow and ice caused by warming during the MWP provided a favorable climatic background for the rapid development of the SR route along the northern slopes of the Tianshan Mountains. The intensification of aeolian activity and the decrease in meltwater supply induced by the LIA cooling had an important impact on the decline of the SR, marked by the closure of the Jiayuguan Pass.

It should be pointed out, high-quality single-site temperature records from the arid central Asia, where the Silk Road lies, are essential for synthesizing the general pattern of temperature changes over the past 2000 years, for evaluating the amplitude of recent warming from a historical perspective, and for analyzing the influence of hydroclimatic changes on the vicissitudes of civilization. The 10 records selected in this study are all from mountain ranges, including the Altai Mts., Qilian Mts., Tianshan Mts., Kunlun Mts., and Karakoram Mts., as shown in Figure 1. The most likely explanation is that most proxies in arid basins are restricted by precipitation/humidity, while precipitation/humidity is not a limiting factor in pluvial mountainous areas and the signals of temperature change can be preserved. Thus, selecting study sites in rainy mountains to diminish the impact of precipitation/humidity variations, or utilizing novel proxies (e.g., iGDGTs) less influenced by precipitation/humidity variations in arid basins, is a prerequisite for obtaining high-quality palaeotemperature reconstructions.

Finally, we suggest that future Holocene paleoclimate research in this region should address the following important questions:

(1) What was the history of temperature change during the period of AD 1–1000 in the eastern part of the SR?

Among the ten records used in this study, only four records completely cover the period of AD 1–1000, which is likely insufficient to average out local variability and identify a regional climate signal. Studies applying the same proxy at different sites that are sensitive to temperature changes and have a clear seasonal significance (e.g., chironomids) can be used to examine the presence of local signals during the first millennium and reveal the definite process of temperature variation in the eastern part of the SR. Furthermore, there were two intervals when the SR flourished within this period: the Han Dynasty and Sui-Tang Dynasties (Chen et al., 2019b). As mentioned above, the significant differences among the existing temperature records have led to contradictions in interpretations of the water resources change in the ancient oasis cities of the Tarim Basin, such as during the 3rd–5th centuries AD. Therefore, clarifying the temperature variations in the study area during the period of AD 1–1000 will continue to a better understanding of the impacts of environmental change on the development of the Silk Road.

(2) What was the combination of heat and water in the eastern part of the SR during the period of AD 1–1000?

The combination of heat and water is an important aspect of hydroclimatic research, and it is also a critical factor in sustainable development in arid regions (Feng et al., 2019). Although meteorological observations indicate a warming and wetting climate in Xinjiang (Yao et al., 2022), proxy records indicate a typical warm-dry/cold-wet climatic pattern in this region over the past millennium (Chen et al., 2015, 2019a and this study). Whether climate change in the study area was still characterized by a warm-dry/cold-wet pattern during the period AD 1–1000, and whether there was warming and wetting climate on the interdecadal scale, remain unclear. Answering these questions may improve our understanding of the combination of climatic factors on multiple time scales under different driving mechanisms, as well as make a theoretical contribution to the environmental change dynamics in this arid region.

(3) How did the temperature change in the western part of the SR over the past 2000 years, and what were the impacts of temperature fluctuations on the vicissitudes of the ancient civilizations?

The western part of the SR passes through Central Asia and West Asia before reaching the Mediterranean region (Figure 1a). No terrestrial proxy records from this region are incorporated in the recent global integration studies (e.g., Neukom et al., 2019; PAGES 2k Consortium, 2013). Existing studies including of the western part of the SR are based mainly on spare data from Eastern and Central Europe on the northern shores of the Mediterranean, and they are generally less than 1000 years in length (e.g., Glaser and Riemann, 2009; Hao et al., 2020). Hence, there is an urgent need to expand the spatio-temporal coverage of high-quality paleoclimate reconstructions and to elucidate the temperature variations in Central and Western Asia (the region hosting the major part of western SR) during the past 2000 years. Moreover, the precipitation in this region is mainly in winter (Hoell et al., 2015; Rana et al., 2019; Xie et al., 2021), and there is a lack of high mountains ('water towers') that can generate large amounts of meltwater, making the relationship between climatic factors (such as temperature and precipitation) and water resources more complicated. Therefore, determining the impact of climatic regimes in this region on the rise and fall of civilizations is the key component of documenting and interpreting the 'panorama' of human-land relationships in the history of the Silk Road.

Acknowledgements *We thank the two reviewers for their constructive comments, and Prof. Haipeng YU, Drs. Jianglin WANG, Wenhuo LIU, and Yanwu DUAN for their data support and valuable suggestions. This work was jointly supported by the National Natural Science Foundation of China (Grant Nos. 41901106, 41822102) and the National Key R&D Program of China (Grant No. 2018YFA0606401).*

References

Aizen E M, Aizen V B, Takeuchi N, Mayewski P A, Grigholm B, Joswiak D R, Nikitin S A, Fujita K, Nakawo M, Zapf A, Schwikowski M. 2016. Abrupt and moderate climate changes in the mid-latitudes of Asia during the Holocene. J Glaciol, 62: 411–439

Babich V V, Rudaya N A, Kalugin I A, Darin A V. 2015. Complex use of the geochemical features of bottom deposits and pollen records for paleoclimate reconstructions (with Lake Teletskoe, Altai Republic, as an example). Contemp Probl Ecol, 8: 405–413

Büntgen U, Myglan V S, Ljungqvist F C, McCormick M, Di Cosmo N, Sigl M, Jungclaus J, Wagner S, Krusic P J, Esper J, Kaplan J O, de Vaan M A C, Luterbacher J, Wacker L, Tegel W, Kirdyanov A V. 2016. Cooling and societal change during the Late Antique Little Ice Age from 536 to around 660 AD. Nat Geosci, 9: 231–236

Chen F H, Chen J H, Holmes J, Boomer I, Austin P, Gates J B, Wang N L, Brooks S J, Zhang J W. 2010. Moisture changes over the last millennium in arid central Asia: A review, synthesis and comparison with monsoon region. Quat Sci Rev, 29: 1055–1068

Chen F, Chen J, Huang W, Chen S, Huang X, Jin L, Jia J, Zhang X, An C, Zhang J, Zhao Y, Yu Z, Zhang R, Liu J, Zhou A, Feng S. 2019a. Westerlies Asia and monsoonal Asia: Spatiotemporal differences in climate change and possible mechanisms on decadal to sub-orbital timescales. Earth-Sci Rev, 192: 337–354

Chen F H, Dong G H, Chen J H, Gao Y Q, Huang W, Wang T, Chen S Q, Hou J Z. 2019b. Climate change and silk road civilization evolution in arid central Asia: Progress and issues (in Chinese). Adv Earth Sci, 34: 561–572

Chen F, Qiang M, Zhou A, Xiao S, Chen J, Sun D. 2013. A 2000-year dust storm record from Lake Sugan in the dust source area of arid China. J Geophys Res Atmos, 118: 2149–2160

Chen G W. 2011. Research on the abandonment of the Dunhuang during Ming Dynasty (in Chinese). J Dunhuang Stud, (1): 111–118

Chen J H, Chen F H, Feng S, Huang W, Liu J B, Zhou A F. 2015. Hydroclimatic changes in China and surroundings during the Medieval Climate Anomaly and Little Ice Age: Spatial patterns and possible mechanisms. Quat Sci Rev, 107: 98–111

Dong G H, Wang L B, Zhang D D, Liu F W, Cui Y F, Li G Q, Shi Z L, Chen F H. 2021. Climate-driven desertification and its implications for the ancient Silk Road trade. Clim Past, 17: 1395–1407

Esper J, Schweingruber F H, Winiger M. 2002. 1300 years of climatic history for Western Central Asia inferred from tree-rings. Holocene, 12: 267–277

Esper J, Shiyatov S G, Mazepa V S, Wilson R J S, Graybill D A, Funkhouser G. 2003. Temperature-sensitive Tien Shan tree ring chronologies show multi-centennial growth trends. Clim Dyn, 21: 699–706

Feng Q, Yang L S, Deo R C, AghaKouchak A, Adamowski J F, Stone R, Yin Z L, Liu W, Si J H, Wen X H, Zhu M, Cao S X. 2019. Domino effect of climate change over two millennia in ancient China's Hexi Corridor. Nat Sustain, 2: 957–961

Feng Z D, Sun A Z, Abdusalih N, Ran M, Kurban A, Lan B, Zhang D L, Yang Y P. 2017. Vegetation changes and associated climatic changes in the southern Altai Mountains within China during the Holocene. Holocene, 27: 683–693

Fu M. 2019. The West Uighur Kingdom on the Silk Road: Study on the History of Eastern Central Asia during the 9th–13th Centuries (in Chinese). Beijing: Social Sciences Academic Press (China)

Ge Q S, Zheng J Y, Fang X Q, Man Z M, Zhang X Q, Zhang P Y, Wang W C. 2003. Winter half-year temperature reconstruction for the middle and lower reaches of the Yellow River and Yangtze River, China, during the past 2000 years. Holocene, 13: 933–940

Ge Q, Hao Z, Zheng J, Shao X. 2013. Temperature changes over the past 2000 yr in China and comparison with the Northern Hemisphere. Clim Past, 9: 1153–1160

Glaser R, Riemann D. 2009. A thousand-year record of temperature variations for Germany and Central Europe based on documentary data. J Quat Sci, 24: 437–449

Hao Z X, Zheng J Y, Yu Y Z, Xiong D Y, Liu Y, Ge Q S. 2020. Climatic changes during the past two millennia along the Ancient Silk Road. Prog Phys Geography-Earth Environ, 44: 605–623

Harris I, Osborn T J, Jones P, Lister D. 2020. Version 4 of the CRU TS monthly high-resolution gridded multivariate climate dataset. Sci Data, 7: 109

He Y X, Zhao C, Song M, Liu W G, Chen F H, Zhang D, Liu Z H. 2015. Onset of frequent dust storms in northern China at ~AD 1100. Sci Rep, 5: 17111

He Y X, Zhao C, Wang Z, Wang H Y, Song M, Liu W G, Liu Z H. 2013. Late Holocene coupled moisture and temperature changes on the northern Tibetan Plateau. Quat Sci Rev, 80: 47–57

Hoell A, Shukla S, Barlow M, Cannon F, Kelley C, Funk C. 2015. The forcing of monthly precipitation variability over Southwest Asia during the boreal cold season. J Clim, 28: 7038–7056

Huang J P, Yu H P, Dai A G, Wei Y, Kang L T. 2017. Drylands face potential threat under 2°C global warming target. Nat Clim Change, 7: 417–422

Huang X Z, Chen C Z, Jia W N, An C B, Zhou A F, Zhang J W, Jin M, Xia D S, Chen F H, Grimm E C. 2015. Vegetation and climate history reconstructed from an alpine lake in central Tienshan Mountains since 8.5 ka BP. Palaeogeogr Palaeoclimatol Palaeoecol, 432: 36–48

Huang X Z, Oberhänsli H, von Suchodoletz H, Sorrel P. 2011. Dust deposition in the Aral Sea: Implications for changes in atmospheric circulation in central Asia during the past 2000 years. Quat Sci Rev, 30: 3661–3674

Jiang Q F, Ji J F, Shen J, Matsumoto R, Tong G B, Qian P, Ren X M, Yan D Z. 2013. Holocene vegetational and climatic variation in westerly-dominated areas of Central Asia inferred from the Sayram Lake in northern Xinjiang, China. Sci China Earth Sci, 56: 339–353

Kalugin I A, Daryin A V, Babich V V. 2009. Reconstruction of annual air temperatures for three thousand years in Altai region by lithological and geochemical indicators in Teletskoe Lake sediments. Dokl Earth Sci, 426: 681–684

Lan J H, Xu H, Sheng E G, Yu K K, Wu H X, Zhou K G, Yan D D, Ye Y D, Wang T L. 2018. Climate changes reconstructed from a glacial lake in High Central Asia over the past two millennia. Quat Int, 487: 43–53

Li Y, Hu L, Zhao Y T, Wang H P, Huang X Z, Chen G J, Leppänen J J, Fontana L, Ren L L, Shi Z L, Liu B, Zhao H. 2021. Meltwater-driven water-level fluctuations of Bosten Lake in arid China over the past 2,000 years. Geophys Res Lett, 48: e90988

Liu X, Qin D, Shao X, Chen T, Ren J. 2005. Temperature variations recovered from tree-rings in the middle Qilian Mountain over the last millennium. Sci China Ser D-Earth Sci, 48: 521–529

Liu X Q, Herzschuh U, Wang Y B, Kuhn G, Yu Z T. 2014. Glacier fluctuations of Muztagh Ata and temperature changes during the late Holocene in westernmost Tibetan Plateau, based on glaciolacustrine sediment records. Geophys Res Lett, 41: 6265–6273

Liu Y, Zheng J Y, Hao Z X, Zhang X Z. 2021. Regional differences for temperature changes in Medieval Warm Period and Little Ice Age over Europe and Asia (in Chinese). Quat Sci, 41: 462–473

Ma Y F. 2019. Jiayuguan Pass: The only Gateway to the Oasis Silk Road during the Ming Dynasty—A Summary of Jiayuguan and the Silk Road Forum in the Ming Dynasty (in Chinese). China's Borderland History and Geography Studies, 29: 197–201

Moberg A, Sonechkin D M, Holmgren K, Datsenko N M, Karlén W. 2005. Highly variable Northern Hemisphere temperatures reconstructed from low- and high-resolution proxy data. Nature, 433: 613–617

Myglan V S, Oidupaa O C, Vaganov E A. 2012a. A 2367-year tree-ring chronology for the Altai-Sayan region (Mongun-Taiga mountain massif). Archaeol Ethnol Anthropol Eurasia, 40: 76–83

Myglan V S, Zharnikova O A, Malysheva N V, Gerasimova O V, Vaganov E A, Sidorov O V. 2012b. Constructing the tree-ring chronology and reconstructing summertime air temperatures in southern Altai for the last 1500 years. Geogr Nat Resour, 33: 200–207

Neukom R, Steiger N, Gómez-Navarro J J, Wang J, Werner J P. 2019. No evidence for globally coherent warm and cold periods over the preindustrial Common Era. Nature, 571: 550–554

PAGES 2k Consortium. 2013. Continental-scale temperature variability during the past two millennia. Nat Geosci, 6: 339–346

Qiang M R, Chen F H, Zhang J W, Gao S Y, Zhou A F. 2005. Climatic changes documented by stable isotopes of sedimentary carbonate in Lake Sugan, northeastern Tibetan Plateau of China, since 2 ka BP. Chin Sci Bull, 50: 1930–1939

Rana S, McGregor J, Renwick J. 2019. Dominant modes of winter precipitation variability over Central Southwest Asia and inter-decadal change in the ENSO teleconnection. Clim Dyn, 53: 5689–5707

Rao Z G, Guo H C, Cao J T, Shi F X, Jia G D, Li Y X, Chen F H. 2020a. Consistent long-term Holocene warming trend at different elevations in the Altai Mountains in arid central Asia. J Quat Sci, 35: 1036–1045

Rao Z G, Huang C, Xie L H, Shi F X, Zhao Y, Cao J T, Gou X H, Chen J H, Chen F H. 2019. Long-term summer warming trend during the Holocene in central Asia indicated by alpine peat α-cellulose δ^{13}C record. Quat Sci Rev, 203: 56–67

Rao Z G, Shi F X, Li Y X, Huang C, Zhang X Z, Yang W, Liu L D, Zhang X P, Wu Y. 2020b. Long-term winter/summer warming trends during the Holocene revealed by α-cellulose δ^{18}O/δ^{13}C records from an alpine peat core from central Asia. Quat Sci Rev, 232: 106217

Rudaya N, Nazarova L, Novenko E, Andreev A, Kalugin I, Daryin A, Babich V, Li H C, Shilov P. 2016. Quantitative reconstructions of mid- to late Holocene climate and vegetation in the north-eastern Altai Mountains recorded in Lake Teletskoye. Glob Planet Change, 141: 12–24

Shao Y, Gong H Z, Elachi C, Brisco B, Liu J Q, Xia X C, Guo H D, Geng Y Y, Kang S G, Liu C A, Yang Z, Zhang T. 2022. The lake-level changes of Lop Nur over the past 2000 years and its linkage to the decline of the ancient Loulan Kingdom. J Hydrol-Regional Studies, 40: 101002

Sun A Z, Feng Z D, Ran M, Zhang C J. 2013. Pollen-recorded bioclimatic variations of the last ~22,600 years retrieved from Achit Nuur core in the western Mongolian Plateau. Quat Int, 311: 36–43

Thompson L G, Yao T, Davis M E, Henderson K A, Mosley-Thompson E, Lin P N, Beer J, Synal H A, Cole-Dai J, Bolzan J F. 1997. Tropical climate instability: The last glacial cycle from a Qinghai-Tibetan ice core. Science, 276: 1821–1825

Thompson L G, Mosley-Thompson E, Brecher H, Davis M, León B, Les D, Lin P N, Mashiotta T, Mountain K. 2006. Abrupt tropical climate change: Past and present. Proc Natl Acad Sci USA, 103: 10536–10543

Wu D D, Cao J T, Jia G D, Guo H C, Shi F X, Zhang X P, Rao Z G. 2020. Peat brGDGTs-based Holocene temperature history of the Altai Mountains in arid Central Asia. Palaeogeogr Palaeoclimatol Palaeoecol, 538: 109464

Xie T T, Huang W, Chang S Q, Zheng F, Chen J H, Chen J, Chen F H. 2021. Moisture sources of extreme precipitation events in arid Central Asia and their relationship with atmospheric circulation. Int J Climatol, 41: E271–E282

Yang B, Braeuning A, Johnson K R, Shi Y F. 2002. General characteristics of temperature variation in China during the last two millennia. Geophys Res Lett, 29: 38-1–38-4

Yao J Q, Chen Y N, Guan X F, Zhao Y, Chen J, Mao W Y. 2022. Recent climate and hydrological changes in a mountain-basin system in Xinjiang, China. Earth-Sci Rev, 226: 103957

Yao T D, Thompson L G, Qin D H, Tian L D, Jiao K Q, Yang Z H, Xie C. 1996. Variations in temperature and precipitation in the past 2000 a on the Xizang (Tibet) Plateau—Guliya ice core record. Sci China Ser D-Earth Sci, 39: 425–433

Yong J C. 2015. History of the Silk Roads (in Chinese). Xi'an: Sanqin Publishing House. 303

Zhang D L, Chen X, Li Y M, Zhang S R. 2020. Holocene vegetation dynamics and associated climate changes in the Altai Mountains of the Arid Central Asia. Palaeogeogr Palaeoclimatol Palaeoecol, 550: 109744

Zhang H, Werner J P, García-Bustamante E, González-Rouco F, Wagner S, Zorita E, Fraedrich K, Jungclaus J H, Ljungqvist F C, Zhu X H, Xoplaki E, Chen F H, Duan J P, Ge Q S, Hao Z X, Ivanov M, Schneider L, Talento S, Wang J L, Yang B, Luterbacher J. 2018. East Asian warm season temperature variations over the past two millennia. Sci Rep, 8: 7702

Zhang H, Zhang Y, Kong Z C, Yang Z J, Li Y M, Tarasov P E. 2015. Late Holocene climate change and anthropogenic activities in north Xinjiang: Evidence from a peatland archive, the Caotanhu wetland. Holocene, 25: 323–332

Zhang Y Q, Luo Y, Sun L, Liu S Y, Chen X, Wang X L. 2016. Using glacier area ratio to quantify effects of melt water on runoff. J Hydrol, 538: 269–277

Zhang Y, Shao X M, Yin Z Y, Wang Y. 2014. Millennial minimum temperature variations in the Qilian Mountains, China: Evidence from tree rings. Clim Past, 10: 1763–1778

Zhang Y, Yang P, Tong C, Liu X T, Zhang Z Q, Wang G P, Meyers P A. 2018. Palynological record of Holocene vegetation and climate changes in a high-resolution peat profile from the Xinjiang Altai Mountains, northwestern China. Quat Sci Rev, 201: 111–123

Zhang Y, Kong Z C, Yan S, Yang Z J, Ni J. 2009. "Medieval warm period" on the northern slope of central Tianshan Mountains, Xinjiang, NW China. Geophys Res Lett, 36: L11702

Zhao C, Liu Z H, Rohling E J, Yu Z C, Liu W G, He Y X, Zhao Y, Chen F H. 2013. Holocene temperature fluctuations in the northern Tibetan Plateau. Quat Res, 80: 55–65

Zhou G P, Huang X Z, Wang Z L, Zhang J, Xie H C. 2019. Eolian activity history reconstructed by Bosten Lake grain size data over the past ~2 000 years (in Chinese). J Desert Res, 39: 86–95

Zhou W Z, Ding J T. 2006. Dictionary of the Silk Road (in Chinese). Xi'an: Shaanxi People's Publishing House

(Responsible editor: Bao YANG)